Oil & Gas Science and Technology – Rev. IFP Energies nouvelles **76**, 1 (2021)

https://doi.org/10.2516/ogst/2020083

Available online at:
ogst.ifpenergiesnouvelles.fr

REGULAR ARTICLE OPEN ACCESS

Elemental geochemistry of the Upper Cretaceous reservoir and surrounding formations applied in geosteering of horizontal wells, Lebăda Field – Western Black Sea

Ionuţ Mihai Prundeanu[1,2], Ciprian Chelariu[3,*], and David Rafael Contreras Perez[4]

[1] University of Bucharest Research Institute (ICUB) – Earth, Environmental and Life Sciences Division, 36–46 Bd. M. Kogălniceanu, 050107 Bucharest, Romania
[2] OMV Petrom, Petrom City, 22 Coralilor Street, 013329 Bucharest, Romania
[3] Department of Geology, "Alexandru Ioan Cuza" University of Iaşi, 20A Carol I Blv., 700505 Iaşi, Romania
[4] OMV Middle East & Africa GmbH, C2 Tower, 15th Floor, 45868 Abu Dhabi, UAE

Received: 1 September 2020 / Accepted: 15 October 2020

Abstract. The precise landing and steering of horizontal wells using conventional mudlogging and Logging While Drilling (LWD) data is a particular challenge for the Lebăda Field, offshore Romania. The use of a new technique of elemental geochemistry analysis (or chemosteering) became an option for the identification of Cenomanian, Turonian–Coniacian–Santonian, Campanian and Eocene strata. This has enabled more accurate placement of the horizontal development wells within the desired reservoir target interval. Geochemical data enabled the identification of chemostratigraphic zones C1, C2, C3 and zone R that correspond to the reservoir section. The application is a result of the geochemical zonation performed using elements and ratios that are sensitive to depositional environment, sea level change, heavy mineral concentrations and siliciclastic input namely: Sr/Ca, Zr/Th, Si/Zr and Si/K. In ascending stratigraphic order, the ratio thresholds of zone C3 are $Zr/Th > 11$, $Sr/Ca > 1.1$, $Si/Zr < 22$ and $Si/K < 19$, while zone R corresponds to $5.5 < Zr/Th < 11$, $Sr/Ca < 1.1$, $Si/Zr > 22$ and $Si/K > 19$. C2 zone is defined by $Zr/Th < 5.5$, $Sr/Ca > 1.1$, $Si/Zr < 22$ and $Si/K < 19$ and C1 zone is characterized by $Si/Zr > 22$ and $Si/K > 19$. The selected geochemical ratios indicate a strong geochemical zonation. In the case of offset wells, 85.9% of the data confirmed the proposed classification and 89.4% for the real-time application case. The zone R shows a strong contrast with the surrounding formations facilitating critical decisions during well placement and geosteering, increasing the reservoir exposure by 28%. The quantitative approach delivered very valuable results, providing a solid foundation to define correlation and well landing intervals. Simultaneously, the cost of the method represents a fraction of the LWD cost and 0.15% of the total project cost, making it very cost effective and a standard approach for future projects.

1 Introduction

For well placement purposes, cuttings elemental composition is rarely used. Generally, for the landing and steering of wells, the industry uses lithology, micropaleontology, real-time petrophysics interpretation from Logging While Drilling (LWD), and gas chromatography data. In the Lebăda Field, offshore in Black Sea (Fig. 1), however, none of these methods enables clear contrast between the reservoir and overlying/underlying sediments (Fig. 2). In order to land horizontal wells for further field development, alternative solutions are necessary.

Chemostratigraphy involves the identification of the geological characteristics based on the spatial-temporal variation of the chemical elements in rocks or the various ratios between these elements (Ramkumar, 2015). Elemental chemostratigraphy can be used as an independent method or in conjunction with other information, such as lithological, geophysical, petrographical and biostratigraphical data. The use of elemental chemostratigraphy at the wellsite is a relatively new development commencing in 2000 (Craigie, 2018), aimed primarily at lithology/mineralogy prediction, placing casing points, coring points and for well trajectory monitoring (geosteering). The major advantage of using elemental chemostratigraphy is its real-time application. Zeriek (2013), points out two chemosteering applications, "reactive" and "proactive", depending on the specific stratigraphic characteristics and the resolution at which it is applied. Reactive application concerns correcting the well's trajectory when the geochemical

* Corresponding author: ciprian.chelariu@uaic.ro

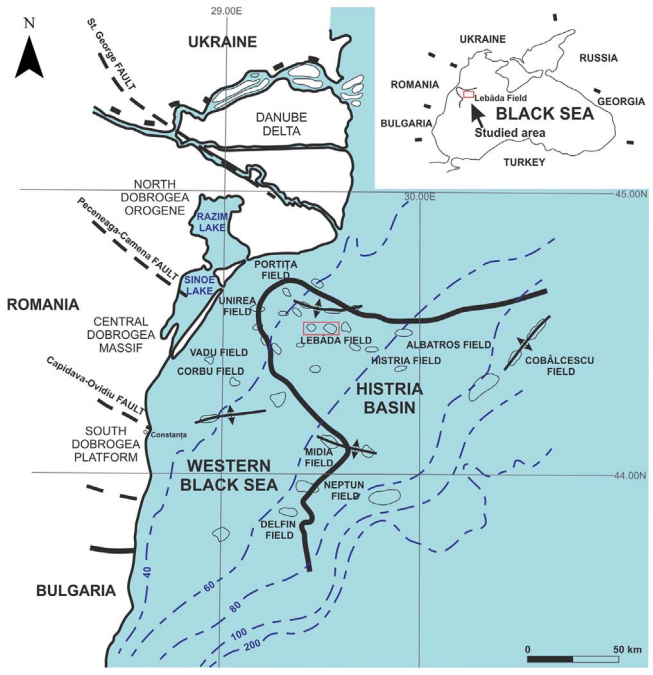

Fig. 1. Map showing the location of the Lebăda field in the Western Black Sea, modified after Șaramet *et al.* (2008) and Crânganu *et al.* (2009).

information indicates an exit from the interest zone. While proactive application involves the identification of distinct elemental trends in a particular chemostratigraphic units in order to react before the bit exits the target formation.

Even though major oil companies use the method, there are very few studies dealing with this subject in the literature. The use of high-resolution elemental chemostratigraphy on existing samples allowed reservoir zonation in a study of carbonate rocks in a Cretaceous reservoir from Minagish, Kuwait (El Gezeery *et al.*, 2009). This helped in the geosteering process, of subsequent wells, including the real-time identification of faults (based on rapid changes of MgO/CaO, S, $(Ni + V + Fe_2O_3)/Al_2O_3$, Na_2O, and Cl).

One of the first chemosteering applications in unconventional reservoirs took place in the North Sea (Pitcher and Jackson, 2012). In such reservoirs, the information obtained from standard Logging While Drilling (LWD) logs and lithological description of cuttings samples were unsatisfactory. However, the elemental geochemistry had the capacity to capture the smallest changes in real-time of the elemental composition of rocks drilled. This allowed the effective detection of faults much more rapidly and clearly than in the more standard conventional mudlogging techniques. Carugo *et al.* (2013) highlighted, among other aspects, the economic benefits of using chemostratigraphy in real time for horizontal drilling.

El Gezeery *et al.* (2013) used chemostratigraphy in the drilling of the first "smart multi-lateral well" in Kuwait and the Middle East Region. This case study describes a heterogeneous Cretaceous reservoir, characterized by channel sandy deposits, crossed by a fault system connected to an aquifer. The geosteering integrated LWD data and the geochemical analyses carried out in real-time on cuttings samples. Elemental geochemistry integration in the process of geosteering allowed the horizontal drilling in the sections with the best reservoir properties. The successful identification of certain faults based on Al, Zr, Ti, and K, led to the isolation of the faulted and poor reservoir quality intervals.

In a case study on the Berea Sandstone Formation (Kentucky, USA), Stypula *et al.* (2016), refered to the growing popularity of the elemental geochemistry in the oil industry and highlighted the importance of chemosteering for checking the stratigraphic position of the borehole, especially in those areas where the gamma-ray curve does not give enough contrast. El Gezeery *et al.* (2017) recommended using chemosteering as an integral part of the geosteering process in complex reservoirs.

In a recent study, Mejia *et al.* (2018) created a model that integrates LWD data with the analysis of core and cuttings samples for geosteering inside target formations. They used the abundance of certain elements or ratios (As/Cr, Mg/Mn, SiO_2/Al_2O_3 and Ga/Rb) for geosteering into those intervals within the reservoir characterized by low natural radioactivity and low resistivity contrast.

Whilst some research has been carried out on cuttings geochemistry applications in well placement and geosteering, no research has been conducted on the quantitative application of geochemical proxies/ratios as a method to differentiate between the target interval and surrounding strata. The present study focuses on the geochemical characterization of the Cenomanian, Turonian–Coniacian–Santonian, Campanian and Eocene strata in three offset wells (Fig. 2). Compared to the classical approaches used in the industry, this paper introduces the use of geochemical data from cuttings as a more precise method for well placement and geosteering of the horizontal wells drilled in the Upper Cretaceous reservoir from Lebăda Field, in the Western Black Sea, Romania. Using selected geochemical ratios in a quantitative manner, confirmed by the zonation confidence, it becomes possible to anticipate and adjust for the geological model uncertainties. The real-time application of such a technique can greatly facilitate an increase in well placement accuracy as is demonstrated by this case study of the Lebăda Field.

2 Geological setting and stratigraphy

While the deepwater concessions of Romania are only in the early exploration stage (Simmons *et al.*, 2018), the Upper Cretaceous reservoir of the Lebăda Field located offshore Romania was discovered between 1980 and 1985, and is considered one of the most important reservoirs offshore, Romania (Fig. 1). The Lebăda Field lies 45 km eastward from the shoreline, within the shallow Romanian shelf with water depths of approximately 50 m (Bukovac *et al.*, 2009).

The tectonic evolution of the Western Black Sea is complicated, with most of the evidence pointing towards an active rift system during Early Cretaceous time (Dinu *et al.*, 2005; Georgiev, 2012; Konerding *et al.*, 2010; Krézsek *et al.*, 2017; Munteanu *et al.*, 2011; Schleder *et al.*, 2015). However, the relationship of such a rifting setting, with a

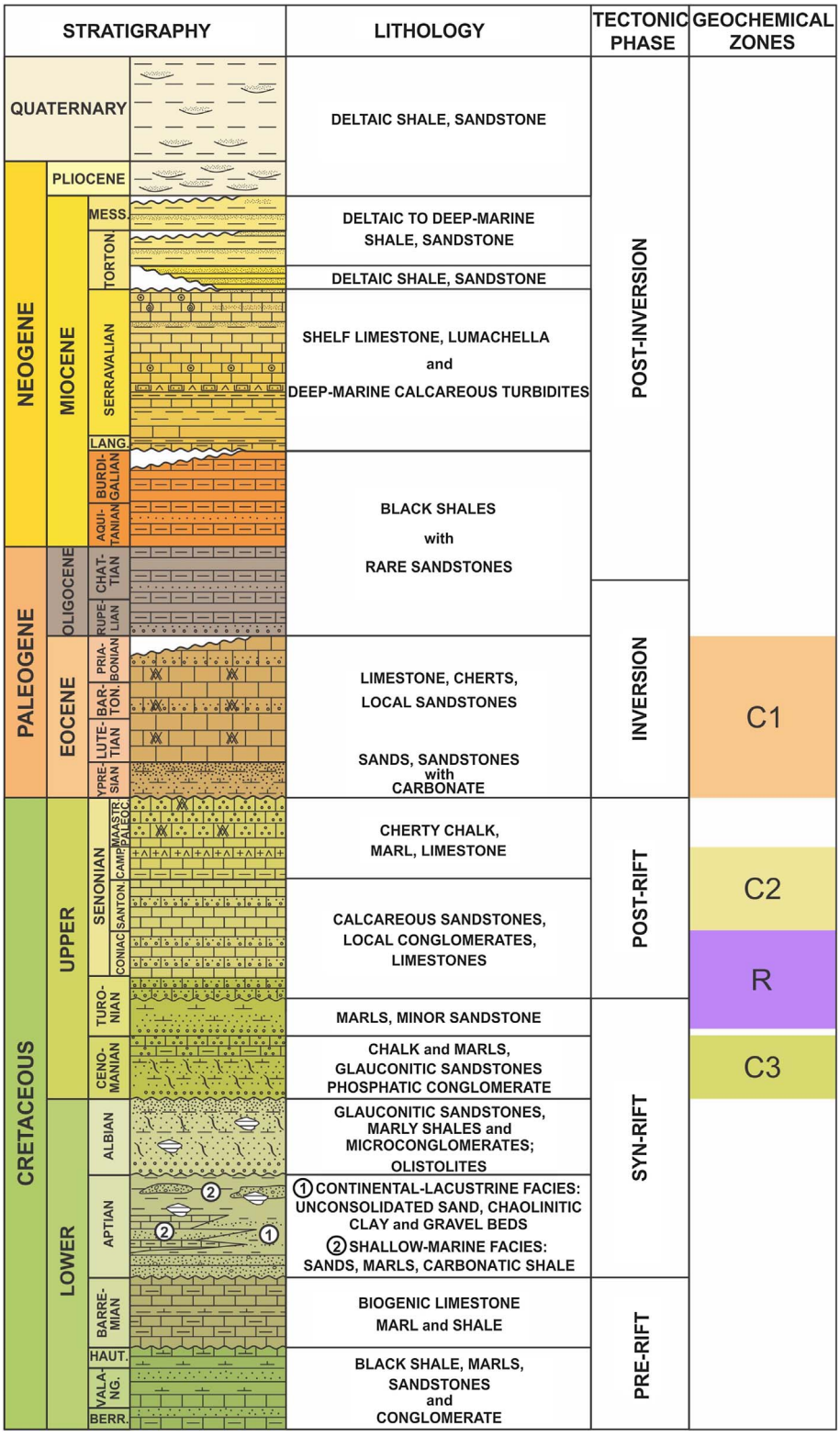

Fig. 2. Stratigraphic chart of the Histria Basin, dominant lithology for each unit described (after Krézsek *et al.*, 2017 and Olaru *et al.*, 2018) and the extent of the C1, C2, R and C3 geochemical zones.

back-arc basin system, is still under discussion and is beyond the scope of the current paper. Additional observations on fault orientations suggest that an extensional fault system developed along the northern active margin of the Tethys Ocean, which subducted northward from the Triassic to Miocene times. Mid-Cretaceous extensional

structures and their sedimentary cover dominate the Romanian Black Sea shelf, subsequently affected by Cenozoic compression (Konerding *et al.*, 2010).

The opening of a back-arc style basin mostly dominated by extensional rifting faults, provides sufficient accommodation space for syn-rift deposits to accumulate from Albian to Cenomanian times (Crânganu *et al.*, 2009; Munteanu *et al.*, 2011). The lateral variations of thickness within the sequences are suggesting a strong syn-tectonic control in the sedimentation across extensional faulting. On the other hand, the deposition of Upper Cretaceous sediments starting in Turonian up to Eocene times is considered to represent a post-rifting sequence. The angular and unconformable relationship between the Upper and Lower Cretaceous suggests a period of non-deposition, with structural tilting, at least in the Romanian offshore area (Krézsek *et al.*, 2017). Figure 2 shows the stratigraphy of the study area from the Lebăda Field with some important information about dominant lithology and tectonic setting.

Regarding hydrocarbon bearing intervals, three different stratigraphic levels are now under production in the study area. Figure 2 summarizes the overall sedimentary section recorded in the Histria Basin, including Lebăda Field. Starting from deep to shallow strata, the target levels are Albian, Upper Cretaceous, and Eocene reservoirs.

The Upper Cretaceous reservoir is a calcareous, post-rift sequence also known as the Santonian–Coniacian–Turonian complex (St–Co–Tu complex). It is a micro-fractured reservoir complex with a mixed carbonate and sandstone lithology (Cațaraiani *et al.*, 2010; Contreras and Sarmiento, 2016). Occasional conglomerates and calcareous-sandstone layers are present at the bottom of the section ranging from 10 to 20 cm thickness up to 5–10 m. At the middle of the section, calcareous-sands and marl intervals overlain by a 30–35 m thick micritic–biogenic–limestone cap-rock dominate the mixture. The targets consist of a thin laminated and tight reservoir with porosity values from 0% up to 25% while permeability ranges from 0.1 to 2.0 mD with an average of 0.8 mD (Bukovac *et al.*, 2009; Cațaraiani *et al.*, 2010; Sofonea *et al.*, 1996).

3 Materials and methods

Samples from three offset wells are the source of the data for the pre-application model. In the well selection process, we took in consideration their position relative to the newly proposed horizontal well, while the final selection depended purely on the historical cuttings samples availability. Washed, dried and grinded cutting samples were analysed for their elemental content. The elemental composition of cuttings resulted from the X-ray fluorescence analysis. The measurement time is short and the method can be deployed on every type of lithology and age. A total of 430 cuttings samples were analysed from wells A, B and C (5 m sampling step) and 662 cutting samples in the real-time application (2.5 m sampling step).

The biggest challenge while sampling wells drilled many years ago is to collect representative samples in terms of lithology percentage of the drilled rock. For offset wells, the authors recommend using any available wireline log to crosscheck the lithology data with the collected samples. For the historical offset wells, the sampling interval was 5 m, conditioned by the sampling rate used at the time of drilling; each collected sample had a weight of 25 g. During the real-time application, to increase the depth resolution and keep up with the pace of the rate of penetration, the chosen sampling step was 2.5 m. At wellsite, the operator is responsible for sample washing and drying. Each sample undergoes a visual check for any contaminants and the removal of any metallic pieces possibly mixed in the cuttings sample during the drilling process with a magnet. In the next step, the samples are ground to fine powder using a dedicated ball mill and put into sample cups, ready for analysis.

Table 1. Detection limits of Olympus Delta ED-XRF.

Elements	Limits of detection
Al, Si	<1%
P	<0.5%
S, Cl	<200 mg/kg
K, Ca, Sc	<50 mg/kg
Ti, V, Cr, Mn, Fe, Co, Ni, Cu, Cd	<10 mg/kg
Zn, Rb, Sr, Zr, Pb, As, Th, U	<5 mg/kg

The sample preparation and analysis take about 10 min, using a portable Olympus Delta EDXRF (Energy Dispersive X-Ray Fluorescence), capable to detect elements from Mg to U (Tab. 1). The EDXRF technique is preferred due to its portability and speed of analysis, critical features for a real-time application. EDXRF is a non-destructive method used to determine the elemental composition of materials. The sample's chemistry results by measuring the fluorescent (or secondary) X-ray emitted from a sample when it is excited by a X-ray source. For extensive information on history and use of portable XRF's, please refer to the work of Lemière (2018). The Olympus Delta EDXRF calibration takes place in the laboratory, using 18 international standards. The onsite calibration is performed using two international standards, SR-1 and JR-1, while a calibration check is carried out every 12 h. The pre-application data and the real-time data are the results of the same preparations process, with the measurements performed with the same apparatus. The data is given as wt. percentage oxides for major elements but, for briefness, the symbol instead of the full oxide is shown in the present article. For example, Ca is quoted, instead of CaO. Trace element concentrations are given in mg/kg. For further information on sample preparation and XRF analysis refer to the work of Craigie (2018).

In many of the studies dealing with chemostratigraphic correlations, different correlation schemes are prepared for the sandstone and mudrock samples (Craigie *et al.*, 2016; Pearce *et al.*, 1999). In the present study, limestone, argillaceous limestone, marl, and calcareous claystone represent most of the lithological components. It is therefore required that the dataset is interpreted in whole. Whereas it is a common practice to avoid the grain size and carbonate dilution influence on the geochemical zonation, focusing

Table 2. Geochemical characterization of zones and the ratios cut offs used to define the zone boundaries.

Zone	Comments	Sr/Ca	Zr/Th	Si/Zr	Si/K
C1	Lower Ca than in C2			>0.22	>19
C2	Higher Mn and Ca than C1 and R	>1.1	<5.5	<0.22	<19
R	Higher Si than in C2	<1.1	>5.5	>0.22	>19
	Sr/Ca minima, Al low to undetectable		<11		
	Generally lower trace elements (Rb, Sr, Cu) than in C2 and C3				
C3	Higher Si than in R and C2	>1.1	>11	<0.22	>19
	Highest Al than in C1, C2 and R				
	Lower Ca than in R and C2				

on the highly resistant elements as provenance indicators, such as Zr, Cr, Y, Hf and other heavy mineral constituents. The main purpose of this study is to divide the Eocene and Cretaceous formations in distinct geochemical zones. Identifying, at field scale, elements and elemental ratios that characterize the economically important zone. Therefore, the use of all available elements is important and necessary, also because the resolution of the portable Olympus Delta EDXRF does not allow the detection of a high range of trace elements, including some of those concentrated in heavy minerals.

Presenting elements and ratios in the form of depth profiles is one of the first steps to define chemostratigraphic zones. After careful screening, a limited number of "key" elements and elemental ratios are selected for chemostratigraphic purposes. The zonation confidence assessment uses the percentage of selected ratios that fall under specifically chosen cut offs (Tab. 2), characteristic for each geochemical zone. The workflow used in the pre-job modelling starts with a general check of the data quality and its descriptive statistical parameters. Together with data plotting in depth profiles, binary and ternary plots help to pick the most useful geochemical proxies. The real-time log uses selected elements and elemental ratios plotted to represent, with the use of different colour shading between curves, changes in the zone boundaries. While drilling, a dedicated team of operators performs the sample collection, preparation and analysis. As soon as new data becomes available, it goes into the model to assess the wellbore trajectory position relative to the target interval.

4 Results and discussion

The utilized XRF apparatus provides data for 25 elements (Tab. 1), not all of them were useful for geochemical fingerprinting. Some concentrations were under the limit of detection, while some elements did not show significant variation along the depth profile. In total, 1092 cutting samples were analysed, in both offset wells and the real-time application case.

The pre-application model builds on the data belonging to three offset wells, named well A, B, and C. In descending stratigraphic order, the age succession in our study interval consists of Eocene, Campanian, target formation (Santonian, Coniacian and Turonian) and Cenomanian sediments.

4.1 Geochemical zonation and correlation of A, B, and C wells

Figure 3 shows the mean values of elemental concentrations and ratios for each zone. The geochemical zones are named C1, C2, R and C3 in descending stratigraphic order (Eocene – C1 | Campanian and St–Co–Tu LST series – C2 | St–Co–Tu SST series – R | Cenomanian – C3) characterized in the offset wells (A, B, and C). The following section outlines the elements/ratios used in this study, the main geochemical features of each zone, its statistical confidence and the geochemical correlation between well A, B, and C.

The zones limits have a general correspondence with the geological formations. Zone C1 is covering the lower section of Eocene. C2 covers the Campanian and the LimeSTone (LST) series attributed to the Santonian–Coniacian–Turonian complex. R zone, also called the SandSTone (SST) series, represents the reservoir interval and it is of Santonian–Coniacian–Turonian age, while C3 zone is of Cenomanian age.

Zone C1 consists mainly of grey marls, sometimes silty with limestone intercalations, marked by lower Ca, Sr and Mn concentrations compared to zone C2, while the elements characteristic of the siliciclastic fraction predominate. In zone C2, the dominant lithology is off-white argillaceous limestone with silty marl and quartzitic sandstone intercalations. The carbonates increase in percentage with depth in zone C2; this resulted in a major decrease of the concentrations of other elements, even the carbonate-associated elements, like Sr, are on a decreasing trend indicating a cleaner limestone closer to the lower limit of this zone. The lithology of zone R includes mainly silty marls, argillaceous limestone and rarely quartzitic sandstones with calcareous cement, a mixture that covers all the other descriptions mentioned in zones C1 and C2. Nevertheless, the elemental geochemistry is able to highlight the differences between zones, Si content is higher; the carbonate is lower in percentage compared to zone C2, and, with the exception of Zr, most of the other major and trace elements have lower concentrations compared to the surrounding

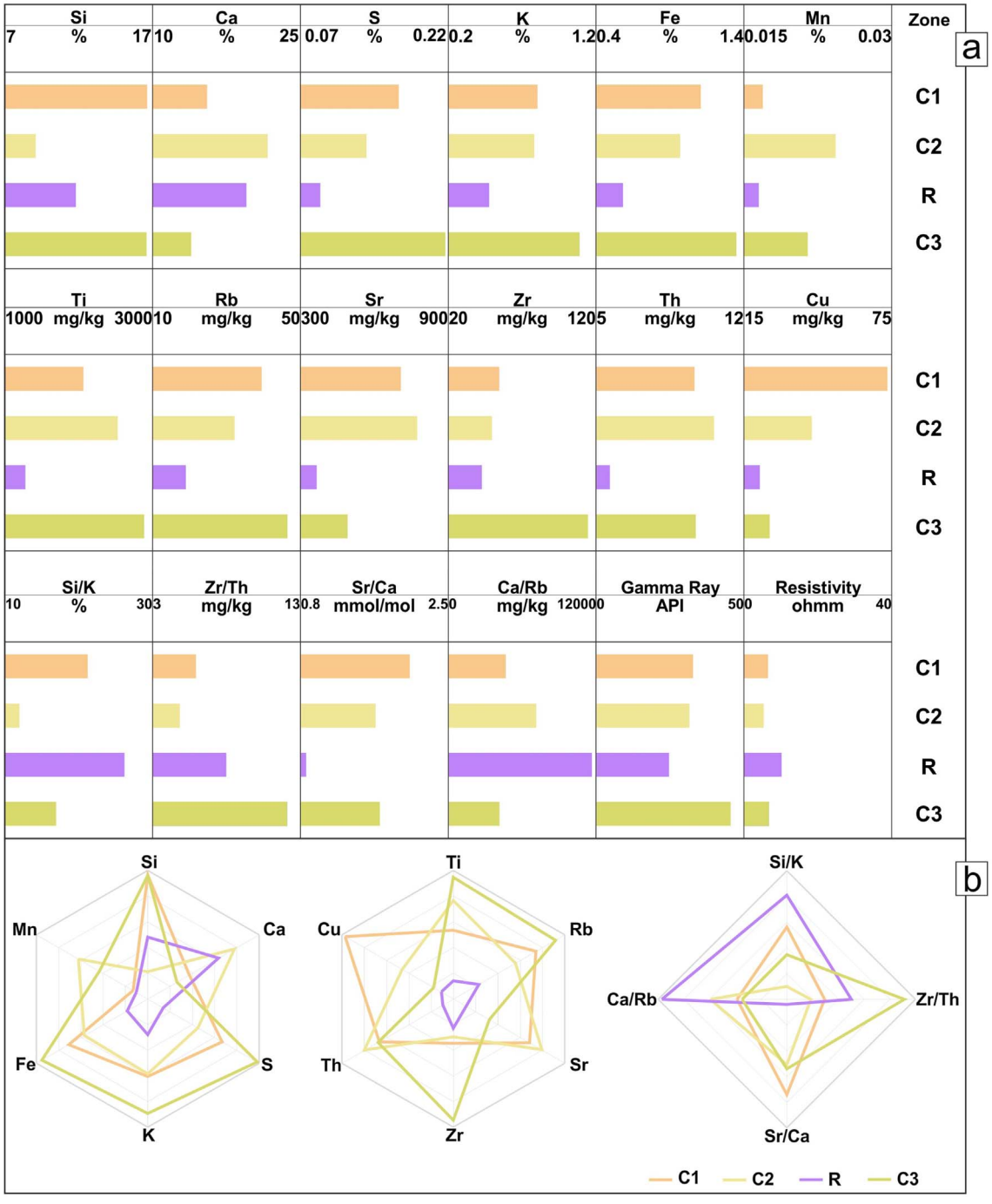

Fig. 3. Mean elemental concentrations of C1 (Eocene), C2 (Campanian and Santonian–Coniacian–Turonian LST series), R (Campanian and Santonian–Coniacian–Turonian SST series) and C3 (Cenomanian) zone. (a) Bar charts plotted as per the in-situ stratigraphic order; (b) radar charts showing the fingerprint characteristic to each zone, the scale of each item plotted on the radar charts is the same to the one used in the bar charts. The use of radar plots have made possible the 2D data visualization of the mean concentrations from each zone. This plot easily helps to distinguish the R zone from the other zones in the study on a visual level. R zone has lower trace element concentrations compared to the surrounding formation. The opposite is valid for major elements like Si and Ca, which accumulate in the R zone, indicating a cleaner limestone with a possible biogenic sourced Si, confirmed by the fingerprint of the ratios radar diagram, where Ca/Rb and Si/K ratios plot distinctively higher compared to the one from C1, C2 and C3 zones.

formations. Silty grey marls with quartzitic sandstone levels are predominant in zone C3. The elemental concentrations confirm the transition from zone R, with higher concentrations for the clay minerals bearing elements (Al, K, Rb, and Fe) and the lowest Ca content of the four zones from this study.

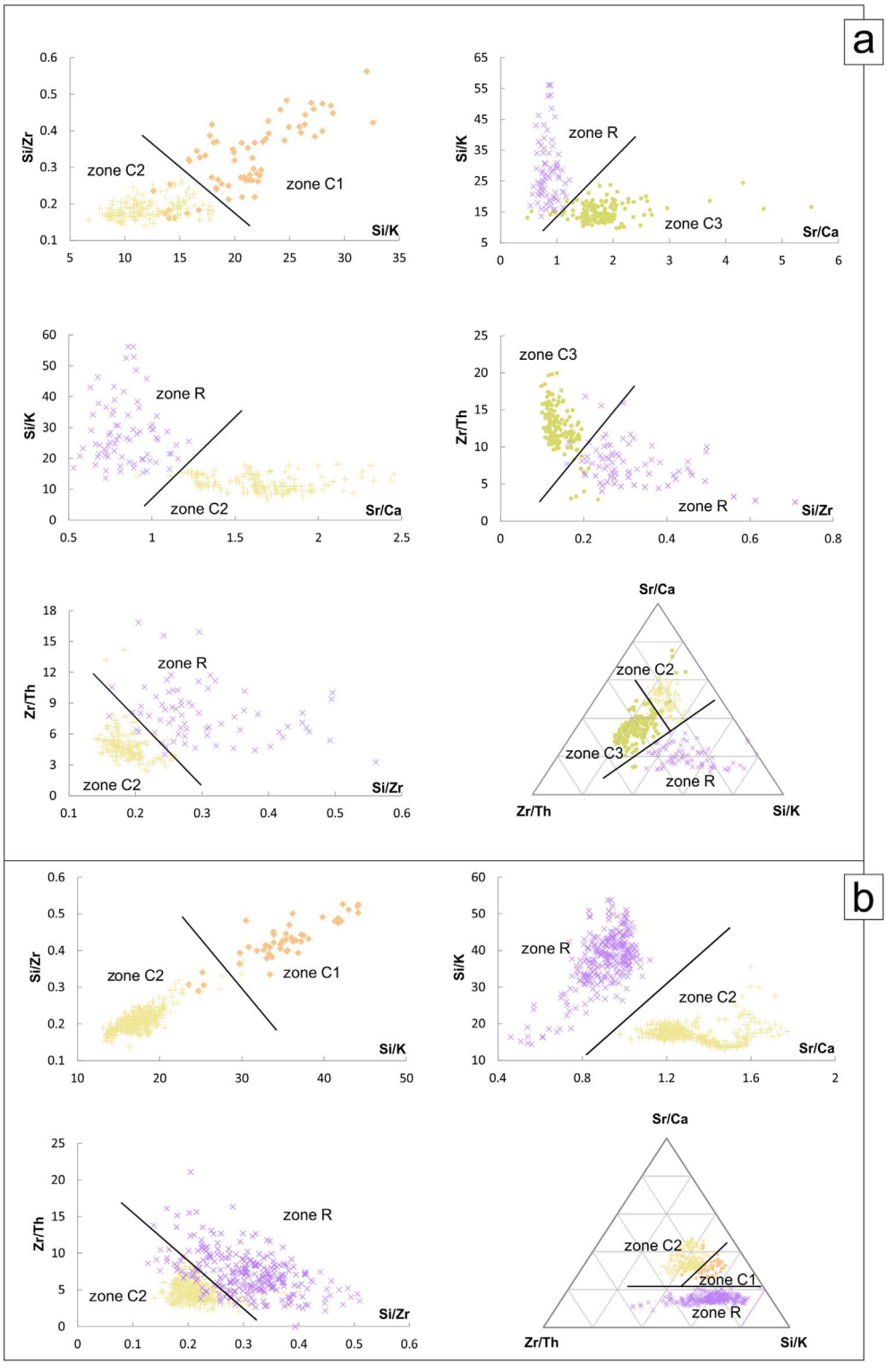

Fig. 4. Binary and ternary diagrams of selected ratios used in the zonation step. (a) For C1, C2, R and C3 in A, B and C wells; (b) for C1, C2, R and C3 in well Z.

4.1.1 Geochemical zones

Higher Si/Zr and Si/K ratios than in C2 and C3, with higher Sr/Ca ratio compared to the R zone are characteristic to zone C1. The geochemical data of zone C2 yield lower Zr/Th, Si/Zr and Si/K ratios and a positive excursion of Sr/Ca ratio compared to zone R. The target zone of the Upper Cretaceous reservoir shows higher Si/Zr

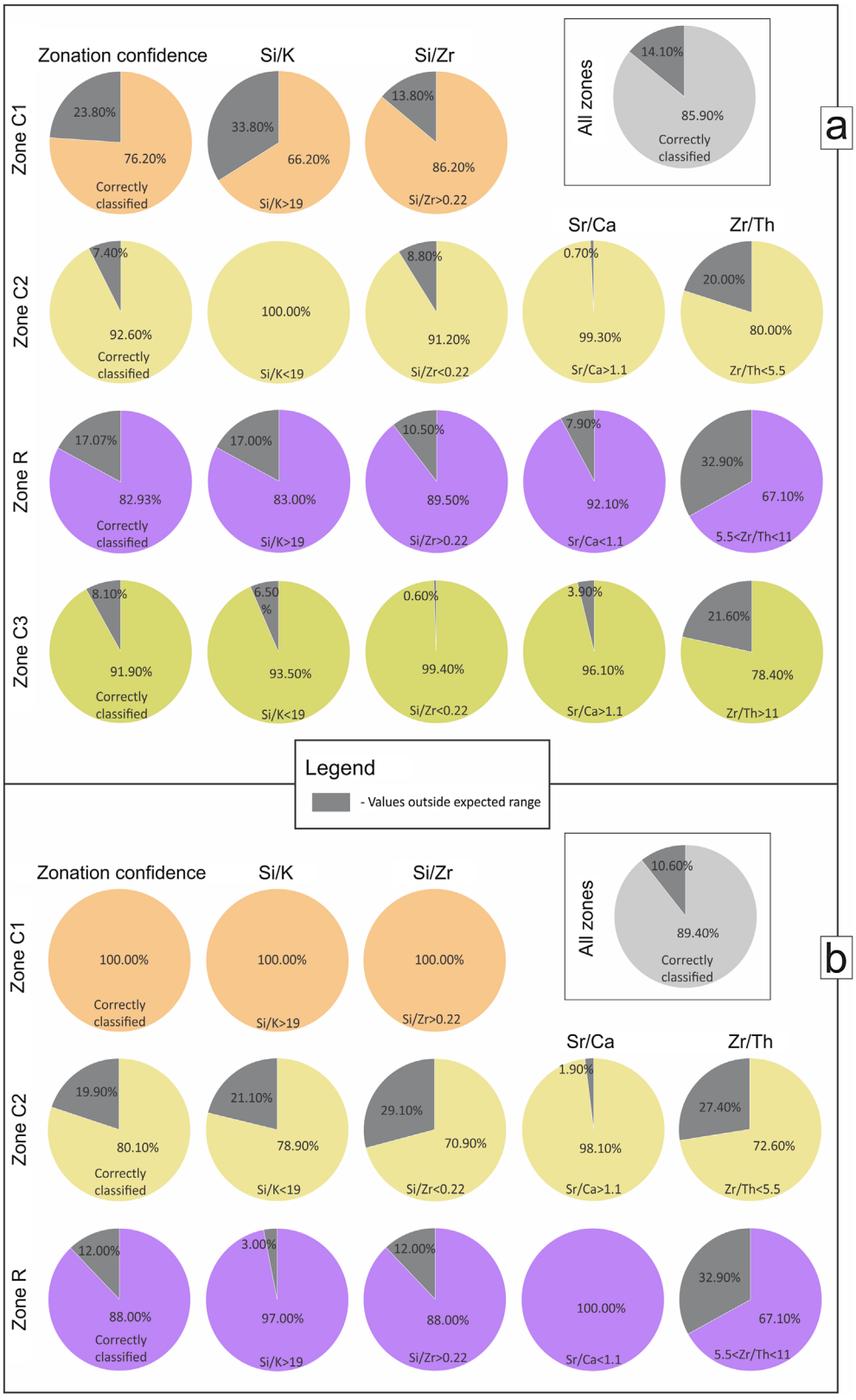

Fig. 5. Pie charts representing the zonation confidence in the defined geochemical zones. (a) A, B and C wells; (b) well Z.

and Si/K and Sr/Ca ratios compared to zone C3. Selected binary and ternary diagrams confirm the proposed zonation (Fig. 4a).

4.1.2 Zonation confidence

Pie charts help to quantify and visualize the zonation confidence. The results show the proportion of samples correctly assigned to each zone considering the cut off used for the key elemental ratio (Fig. 5a).

Samples assigned to zone C1 yield an average of 76.2% data correctly classified. The percentage of C1 zonation, for Si/K > 19, is the lowest among the four zones described in the study. Zone C2 has the highest percentage in terms of proxies' correctly classified in the offset wells, average 92.6% with Si/K, Sr/Ca and Si/Zr ratios over 90% successfully attributed to zone C2. Zone R is described by overall sample classification confidence of 82.9%. The most reliable ratio in terms of accurately describing zone R is Sr/Ca with 92.1% samples correctly classified. Zone C3 is of high importance, as faults under the seismic resolution or geological model uncertainty could result in an unexpected exit from the interest zone during horizontal drilling. For zone C3, the zonation confidence is 91.9%, with values over 90% for Si/Zr, Sr/Ca and Si/K ratios.

The chemostratigraphic zonations have a high level of confidence, with 85.9% of the samples accurately classified in the pre-application stage (Tab. 3). The results are robust, as confidence values over 70% represent a high level of zonation confidence (Craigie, 2016).

Table 3. Zonation confidence for C1, C2, R and C3 zones in A, B and C wells.

Zone	Ratio	% zonation confidence		
		Ratio	Zone	All zones
C1	Si/Zr > 0.22	86.2	76.2	85.9
	Si/K > 19	66.2		
C2	Si/Zr < 0.22	91.2	92.6	
	1.1 < Sr/Ca < 1.6	99.3		
	Zr/Th < 5.5	80		
	Si/K < 19	100		
R	Si/Zr > 0.22	89.5	82.9	
	Si/K > 19	83		
	Sr/Ca < 1.1	92.1		
	5.5 < Zr/Th < 11	67.1		
C3	Si/Zr < 0.22	99.4	91.9	
	Si/K < 19	93.5		
	Sr/Ca > 1.1	96.1		
	5.5 < Zr/Th < 11	78.4		

4.1.3 Chemostratigraphic correlation

Figure 6 shows an overview of the chemostratigraphic correlation, including the geochemical profile of selected ratios between the studied wells. The correlation scheme preparation starts by plotting all the elemental data in a profile. Binary and ternary diagrams of the elements and ratios that show variation along the depth profile help to evaluate the sample distribution and preliminary asses the zonation strength of different geochemical proxies. Subsequently, follows the identification of the key elements and elemental ratios that distinguish between the C1, C2, R and C3 zones with a high level of zonation confidence. The proposed correlation scheme for the three wells is strong, with over 85% zonation confidence. All the four geochemical zones are recognized in A, B and C wells, pointing to a correlation scheme that is accurate for the Lebăda field. The shading between element and elemental ratios curves enhances the visualization of the correlation log between the three offset wells. Changes in shading colour or area are usually indicating a different zone (Fig. 6).

Generally, the geochemical characteristics of the zones show the same variations in all three wells. Zone C1, representing the lower part of the Eocene formation, which has similar features in all the three wells. Above the reservoir is zone C2, covering the Campanian and the so-called limestone series of the Santonian–Coniacian–Turonian, which exhibits a typical downhole pattern of Sr/Ca variation, decreasing with depth. This is a very important aspect because it provides information on well trajectory position proactively which leads to better appreciate the placement with respect to the reservoir interception. Silty marls, limestone and quartzitic sandstone, with a low but noticeable increase in carbonate presence in the EW direction, characterize zone R. At the top of zone R, Zr/Th ratio shows a positive excursion in all the offset wells, Sr/Ca ratio continues the downhole decreasing trend, reaching its minima inside this zone. Generally, the correlation has a layer-cake character, with very few variations from well to well. Zone C3 (Cenomanian), deposited in a syn-rift tectonic setting, has an unmistakable geochemical fingerprint, that allows a clear correlation between the studied wells (Fig. 5a). Sr/Ca and Zr/Th have a clear increase at the top of zone C3, while Si/Zr and Si/K show a strong negative excursion.

4.2 Real-time application

4.2.1 Chemosteering

Low variation characterizes the elemental ratios profiles of the C1 zone. In the base of zone C1, a Si rich layer is present in all three offset wells, signalled by positive excursion of Si/Zr and Si/K ratios. Due to the Si concentration increase, the contents of Ca and Sr are low until we drill through the top of zone C2. A significant positive excursion of Mn concentrations occurs when the well path enters zone C2, accompanied by Si/Zr, Si/K, and Zr/Th ratios negative excursions. Ignoring short-term variation of Sr/Ca, this ratio is on a downhole decreasing trend throughout C2 zone, this characteristic continues in the R zone, where the minima is reached. As the trajectory intercepts the reservoir, the Zr/Th, Sr/Ca, Si/Zr, Si/K ratios excursions on the geosteering log are clearly visible. At this point, the project team decided to land the well and the horizontal section continued through the reservoir.

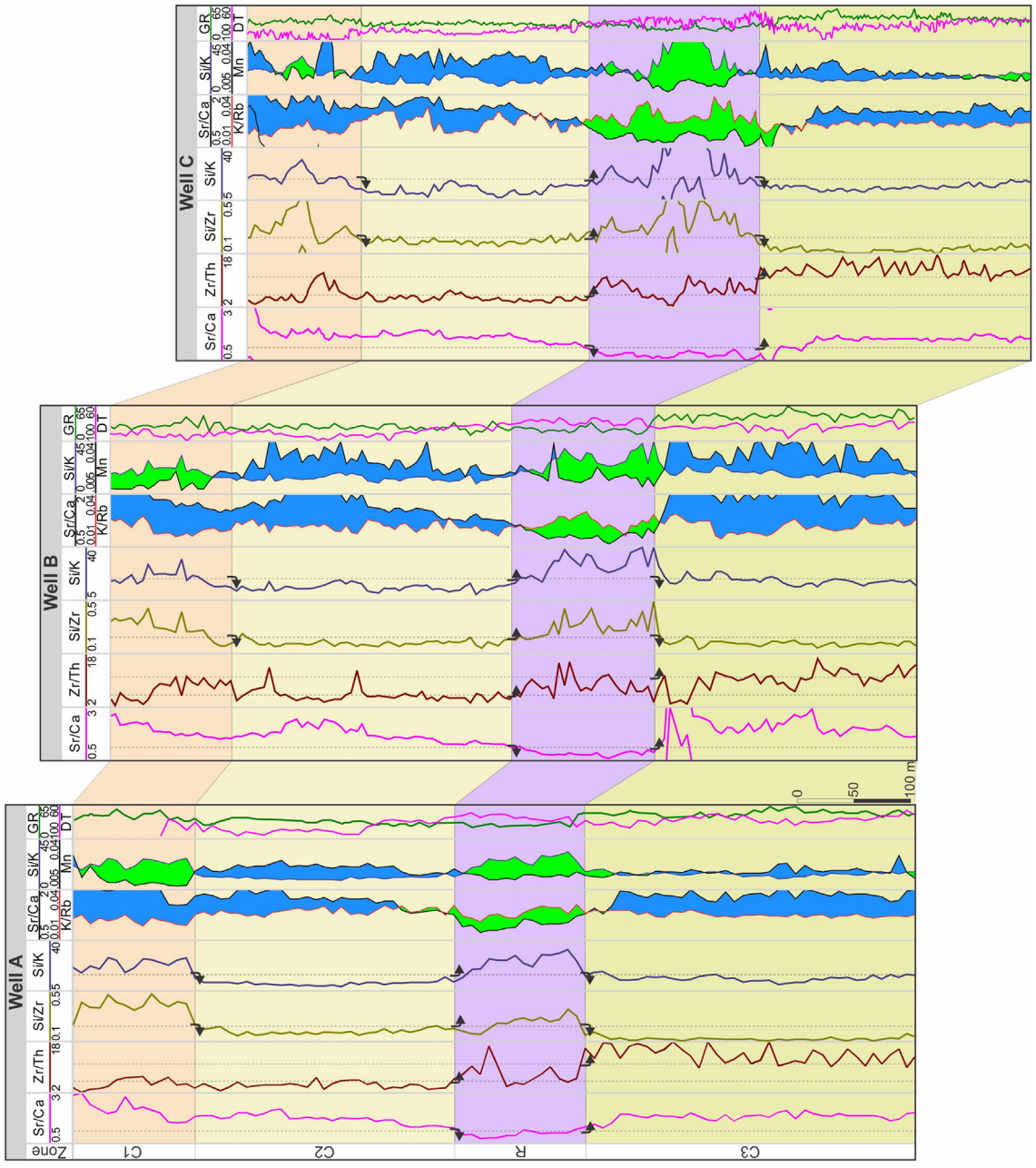

Fig. 6. Chemostratigraphic correlation for A, B and C wells, with the plotted geochemical profiles for Sr/Ca, Zr/Th, Si/Zr, Si/K, K/Rb and Mn. GR – Gamma Ray and DT – acoustic log travel time (sonic log). The transversal dotted lines plotted on each track shows the threshold values used to characterize each geochemical zone.

Total depth of the well Z was 3922 m Measured Depth (MD), out of which 757 m MD drilled into zone R. The geochemical analysis onsite started in Eocene, corresponding to zone C1 with a total of 1622 m covered and 662 samples analysed. Sample lag time plus the analysis time is about 1 h and average rate of penetration was 12–15 m/h.

The geochemical data proved a useful asset as per events described below, contributing directly to drilling decisions taken Figure 7:

1. According to the geological model, the target formation top is at 2871.3 MD (Measured Depth). With no confirmation of zone R from the geochemical data, the team went for decision to drop down the inclination with 3° (from 87° to 84°).
2. Close to 3020 m MD, without a reservoir confirmation by the elemental analysis, a new trajectory adjustment followed, dropping the inclination with another 4° (from 84° to 80°).

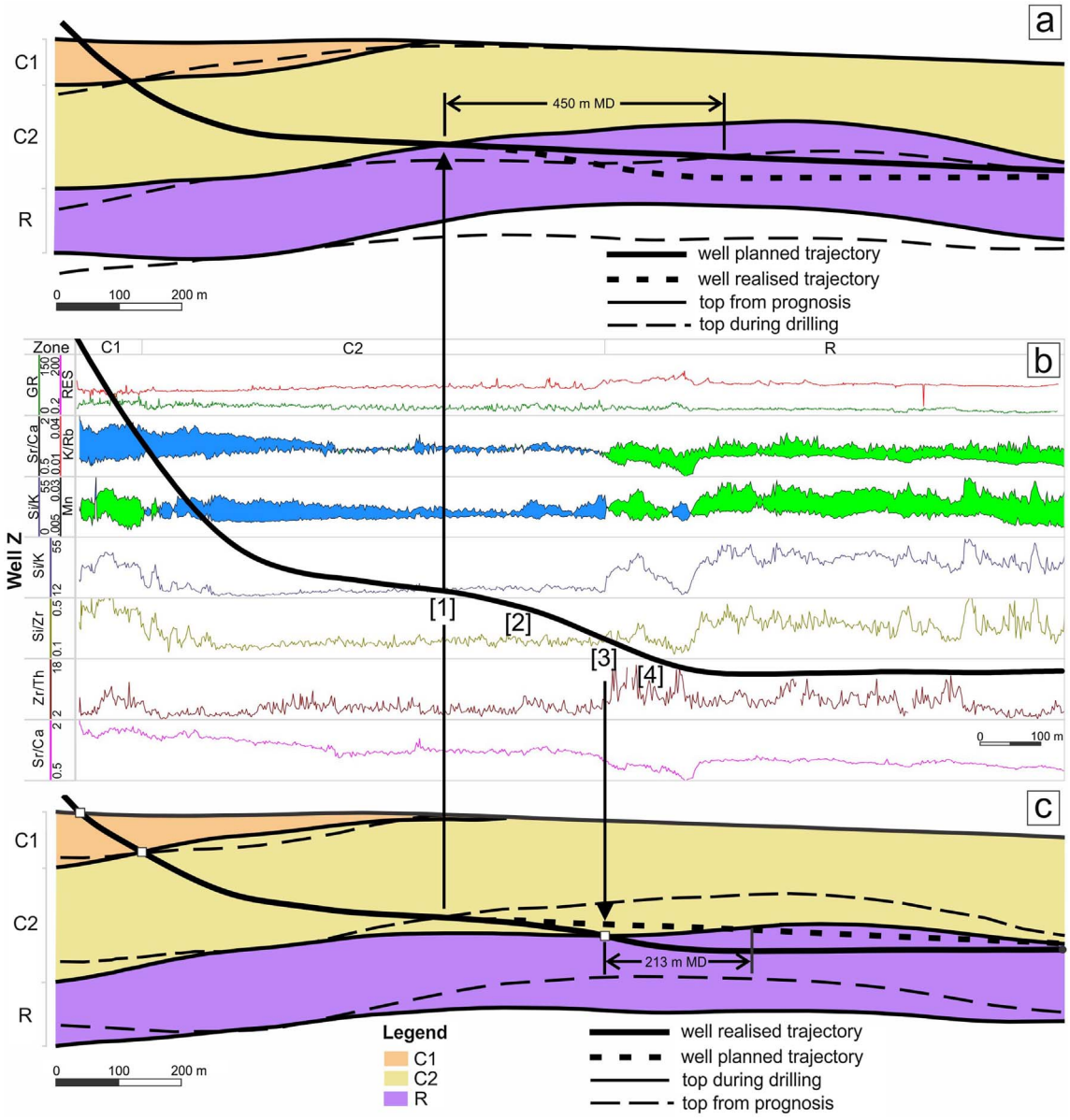

Fig. 7. Chemosteering log and real-time decision facilitated by the use of elemental geochemical analysis. Planned trajectory versus realised trajectory, all depths are in meters. (a and c) Planned trajectory and realised trajectory over the tops from prognosis coloured according to the corresponding zone ((a) coloured as per prognosed tops; (c) coloured as per tops during drilling); (b) geochemical log and the realised well trajectory, with the decision points marked along the wellbore.

3. At 3165 m MD, the geochemical data confirmed the reservoir interception, drilling ahead with the same inclination.
4. After another 55 m MD came the confirmation to be inside zone R, the well trajectory landed on 90°, and drilled ahead to TD.

Using the geochemical data to overcome the uncertainties of the geological model proved to be successful. The vertical difference between the prognosis and the real top of zone R was 30.32 m TVD deeper, most likely due to structural uncertainty from seismic mapping. In a highly inclined well, this can translate in hundreds of meters drilled outside the reservoir. Without any geosteering, if the well trajectory followed the initial plan, approximately 450 m of reservoir section would have been lost, representing 45.3% of the total planned reservoir exposure. Chemosteering application enhanced the fast decision to drop inclination at the right time, entering 213 m MD earlier into zone R, when compared to the initial trajectory. The lateral section gained by the prompt decision to drop the inclination accounts for 28% of the total reservoir exposure of 757 m MD. The elemental geochemistry helped to steer this multi-million EUR well with a financial impact of approximately 0.15% from the total cost of the well and 10% of the LWD investigations cost. In return, supporting

Table 4. Zonation confidence for C1, C2 and R zones in well Z.

Zone	Ratio	% zonation confidence		
		ratio	zone	all zones
C1	$Si/Zr > 0.22$	100	100	89.4
	$Si/K > 19$	100		
C2	$Si/Zr < 0.22$	70.9	80.1	
	$1.1 < Sr/Ca < 1.6$	98.1		
	$Zr/Th < 5.5$	72.6		
	$Si/K < 19$	78.9		
R	$Si/Zr > 0.22$	88	88	
	$Si/K > 19$	97		
	$Sr/Ca < 1.1$	100		
	$5.5 < Zr/Th < 11$	67.1		

decisions of trajectory changes that increased the reservoir exposure by 28% in this particular case.

4.2.2 Zonation confidence for well Z

The method used to identify the C1, C2 and R zones in well Z follows the same steps from the correlation wells zonation. Figure 4b shows binary and ternary plots of the real-time generated data in well Z. The samples from zone C1 correctly classified in the proportion of 100%. In the zone C2, the Sr/Ca ratio was able to assign correctly 98.1% of the data, while the Si/Zr ratio correctly classified 70.9% of the samples. The average zonation confidence of zone C2 was 80.1%. In the reservoir, the Sr/Ca ratio correctly assigned 100% of the samples. Si/Zr and Si/K ratios yield 88% and 97% of samples correctly classified, the average for the zone R being 88%.

Considering the four proxies used in the zonation process, an overall value of 89.4% of the 662 samples of well Z were properly assigned to the correct zone (Fig. 5b, Tab. 4), confirming the consistency of the pre-application geochemical model and the precision of the real-time application of chemosteering.

5 Conclusion

This is the first application of geochemical data in well placement purposes performed in Black Sea and its results validate the method as part of a viable solution when classical approaches do not offer enough dissimilarity between strata. Moreover, the quantitative approach on geochemical ratios proved to be a reliable method for precise characterization of the target interval in contrast to the surrounding strata:

1. The key ratios and elements used to fingerprint the Upper Cretaceous reservoir to Eocene include Sr/Ca, Zr/Th, Mn, Si/Zr, and Si/K; the main controllers of these ratios variation are the depositional environment and the siliciclastic input.
2. The geochemical model consists of four zones, labelled C1, C2, R and C3 in descending stratigraphic order. With C1 characterized by $Si/Zr > 22$ and $Si/K > 19$. C2 is defined by $Zr/Th < 5.5$, $Sr/Ca > 1.1$, $Si/Zr < 22$ and $Si/K < 19$. Zone R corresponds to $5.5 < Zr/Th < 11$, $Sr/Ca < 1.1$, $Si/Zr > 22$ and $Si/K > 19$, while C3 yields $Zr/Th > 11$, $Sr/Ca > 1.1$, $Si/Zr < 22$ and $Si/K < 19$. The proposed zonation derived from chemostratigraphic analysis confirms the current descriptions of the strata, however, the quantitative approach derived from the presented ratios provide a stronger foundation to define correlation and well landing intervals.
3. Binary and ternary diagrams coupled with elemental and ratios profiles are suited to identify the main proxies during the zonation step. The zonation confidence is 85.9% for the three wells analysed in the pre-application step and 89.4% in the real-time application. Hence, confirming the validity of the geochemical model before and after the real-time application.
4. The total cost of the application accounts for 0.15% from the total project budget, and only 10% of the LWD cost. Due to the insignificant cost of the method, which led to very valuable results, the application will be present as standard approach in future drilling campaigns.

Acknowledgments. We thank to *OMV Petrom's Management* and the *Romanian National Agency for Mineral Resources* for allowing us to publish proprietary data. The authors are grateful for the preliminary review of this paper provided by Neil Craigie and for the useful comments that improved the text made by Paul Lyon. This research project has been funded through the ICUB Fellowship for Young Researchers 2017 Call, Project financed by the *Research Institute of the University of Bucharest* (*ICUB*).

References

Bukovac T., Belhaouas R., Perez D.R., Dragomir A., Ghita V., Webel C.E. (2009) Successful multistage hydraulic fracturing treatments using a seawater-based polymer-free fluid system executed from a supply vessel; Lebăda Vest Field, Black Sea Offshore Romania, in: *2009 SPE EUROPEC/EAGE Annual Conference and Exhibition, 8–11 June, Amsterdam, Netherlands*, SPE 121204, 16 p. https://doi.org/10.2118/121204-MS.

Carugo C., Malossi P., Galimberti R., Pingitore F., Previde-Massara E., Rivolta F. (2013) Advanced cuttings analysis improves reservoir characterization and reduces operating times in shale gas drilling project, in: *International Petroleum Technology Conference, 26–28 March, Beijing, China*, IPTC 17186, 15 p. https://doi.org/10.2523/IPTC-17186-MS.

Cațaraiani R., Iosif R., Dragomir A., Perez D.R., Belhaouas R., Emmanuel B., Webel C. (2010) Multidisciplinary workflow applied to multiple stage hydraulic fracturing of horizontal wellbores: Evolving the process in the Lebăda Field, Black Sea, in: *2010 SPE EUROPEC/EAGE Annual Conference and Exhibition, 14–17 June, Barcelona, Spain*, SPE 130786, 12 p. https://doi.org/10.2118/130786-MS.

Contreras D., Sarmiento V. (2016) Estimating lithology in a clastic-carbonate mixed reservoir using seismic inversion and well log data in the Upper-Cretaceous Lebăda field. Black-Sea Romania (Abstract). Petroleum Systems of Alpine-Mediterranean Fold Belts and Basins, in: *AAPG European Regional Conference and Exhibition, 19–20 May, Bucharest, Romania*, Abstract Book, 18 p.

Craigie N.W. (2016) Chemostratigraphy of the Silurian Quisaba Member, Eastern Saudi Arabia, *J. Afr. Earth Sci.* **113**, 12–34. https://doi.org/10.1016/j.jafrearsci.2015.10.007.

Craigie N.W. (2018) *Principles of elemental chemostratigraphy. A practical user guide*. Advances in Oil and Gas Exploration & Production. Berlin, Germany: Springer, 189 p. https://doi.org/10.1007/978-3-319-71216-1.

Craigie N.W., Breurer P., Khidir A. (2016) Chemostratigraphy and biostratigraphy of Devonian, Carboniferous and Permian sediments encountered in eastern Saudi Arabia: An integrated approach to reservoir correlation, *Mar. Petrol. Geol.* **72**, 156–178. https://doi.org/10.1016/j.marpetgeo.2016.01.018.

Crânganu C., Villa M.A., Șaramet M., Zakharova N. (2009) Petrophysical characteristics of source and reservoir rocks in the Histria Basin, Western Black Sea, *J. Petrol. Geol.* **32**, 4, 357–371. https://doi.org/10.1111/j.1747-5457.2009.00455.x.

Dinu C., Wong H.K., Țambrea D., Mațenco L. (2005) Stratigraphic and structural characteristics of the Romanian Black Sea shelf, *Tectonophysics* **410**, 1–4, 417–435. https://doi.org/10.1016/j.tecto.2005.04.012.

El Gezeery T., Hammim A., Zereik R., Simon N., Scheibe C. (2009) A high-resolution chemostratigraphy application in carbonates – Study in the Cretaceous Mishrif Reservoir, Minagish Field, Kuwait, in: *International Petroleum Technology Conference, 7–9 December, Doha, Qatar*, IPTC 13875, 16 p. https://doi.org/10.2523/IPTC-13875-MS.

El Gezeery T., Al Anezi K., Ismael A.A., Silambuchlvan J., Latif A.A., Prakash D.O.M., Padhy G.S., Estarabadi J., Marai N., Shoeibi A., Khan F. (2013) High resolution chemosteering in drilling horizontal wells, Kuwait, in: *SPE Middle East oil and Gas Show and Conference, 10–13 March, Manana, Bahrain*, SPE 164385, 9 p. https://doi.org/10.2118/164385-MS.

El Gezeery T., Al Shemali N., Ebaid A., Kumar J., Padhy K., Das O., Al Rashidi T., Nugroho C., Pazos J.H., Noueihed R.S. (2017) High resolution data integration aid on achieving successful level-4 multilateral wells in clastic reservoirs of Minagish Field, in: *Abu Dhabi International Petroleum Exhibition & Conference, 13–16 November, Abu Dhabi, UAE*, SPE-188855-MS, 21 p. https://doi.org/10.2118/188855-MS.

Georgiev G. (2012) Geology and hydrocarbon systems in the Western Black Sea, *Turk. J. Earth Sci.* **21**, 5, 723–754. https://doi.org/10.3906/yer-1102-4.

Konerding C., Dinu C., Wong H.K. (2010) Seismic sequence stratigraphy, structure and subsidence history of the Romanian Black Sea shelf, *Geol. Soc. Lond. Special Publ.* **340**, 1, 159–180. https://doi.org/10.1144/SP340.9.

Krézsek C., Bercea R.I., Tari G., Ionescu G. (2017) Cretaceous sedimentation along the Romanian margin of the Black Sea: Inferences from onshore to offshore correlations, in: Simmons M.D., Tari G.C., Okay A.I. (eds), *Petroleum geology of the Black Sea*, Geological Society, London, Special Publications, Vol. **464**, pp. 211–245. https://doi.org/10.1144/SP464.10.

Lemière B. (2018) A review of pXRF (Field Portable X-ray Fluorescence) applications for applied geochemistry, *J. Geochem. Explor.* **188**, 350–363. https://doi.org/10.1016/j.gexplo.2018.02.006.

Mejia C., Nardi G., Drew I. (2018) Integration of LWD and geochemistry from cuttings measurements for well placement based on real time diagenesis characterization, in: *Offshore Technology Conference, 30 April–3 May, Houston, Texas, USA*, OTC-29040, 12 p. https://doi.org/10.4043/29040-MS.

Munteanu I., Mațenco L., Dinu C., Cloetingh S. (2011) Kinematics of back-arc inversion of the Western Black Sea Basin, *Tectonics* **30**, 5, 1–21. https://doi.org/10.1029/2011TC002865.

Olaru R., Krézsek C., Rainer T.M., Ungureanu C., Turi V., Ionescu G., Tari G. (2018) 3D basin modelling of Oligocene-Miocene Maikop source rocks offshore Romania and in the Western Black Sea, *J. Pet. Geol.* **41**, 351–365. https://doi.org/10.1111/jpg.12707.

Pearce T.J., Besley B.M., Wray D.S., Wright D.K. (1999) Chemostratigraphy: A method to improve interwell correlation in barren sequences – a case study using onshore Duckmantian/Stephanian sequences (West Midlands, U.K.), *Sediment. Geol.* **124**, 1–4, 197–220. https://doi.org/10.1016/S0037-0738(98)00128-6.

Pitcher J., Jackson T. (2012) Geosteering in unconventional shales: Current practice and developing methodologies, in: *SPE/EAGE European Unconventional Resources Conference and Exhibition, 20–22 March, Vienna, Austria*, SPE-152580, 11 p. https://doi.org/10.2118/152580-MS.

Ramkumar M. (2015) Toward standardization of terminologies and recognition of chemostratigraphy as a formal stratigraphic method (Ch. 1), in: Ramkumar M. (ed), *Chemostratigraphy. Concepts, techniques, and applications*, Elsevier, Amsterdam, 527 p. https://doi.org/10.1016/B978-0-12-419968-2.00001-7.

Șaramet M., Gavrilescu G., Crânganu C. (2008) Quantitative estimation of expelled fluids from Oligocene rocks, Histria Basin, Western Black Sea, *Mar. Pet. Geol.* **25**, 544–552. https://doi.org/10.1016/j.marpetgeo.2007.05.011.

Schleder Z., Tari G., Krezsek C., Kosi W., Turi V., Fallah M. (2015) Regional structure of the Western Black Sea Basin: Constraints from cross-section balancing, in: Post P.J., Coleman J., Rosen N.C., Brown D.E., Roberts-Ashby T., Kahn P., Rowan M. (eds), *Petroleum systems in "Rift" basins*, SEPM, Vol. **34**, pp. 396–411. https://doi.org/10.5724/gcs.15.34.0396.

Simmons M.D., Tari G.C., Okay A.I. (2018) Petroleum geology of the Black Sea: Introduction, in: Simmons M.D., Tari G.C., Okay A.I. (eds), *Petroleum geology of the Black Sea*, Geological Society, London, Special Publications, Vol. **464**, pp. 1–18. https://doi.org/10.1144/SP464.15.

Sofonea R., Spinu S., Smocot I., Tabanescu V., Adamache I. (1996) Horizontal drilling makes possible the development of Lebăda East Oil Field-Upper Cretaceous Formation in the Romanian Continental Shelf of the Black Sea second part: Drilling, completion, and production operations, in: *SPE International Conference on Horizontal Well Technology, 18–20 November, Calgary, Canada*, SPE 37135, 6 p. https://doi.org/10.2118/37135-MS.

Stypula M.J., Blood D.R., Douds A.S.B. (2016) Elemental data collected in the Berea sandstone of Eastern Kentucky: Applications to wellbore placement, horizontal chemosteering and completion strategy (Abstract) AAPG datapages/search and discovery, Art. 90258, in: *AAPG Eastern Section Meeting, 25–27 September, Lexington, Kentuky*, 1 p.

Zeriek R. (2013) Chemosteering using elemental chemostratigraphy (Abstract), AAPG datapages/search and discovery, Art. 90269, in: *AAPG Middle East Region, 25–27 February, Sharm El Sheikh, Egypt*, 1 p.